frontiers | Frontiers in Environmental Science

TYPE Original Research
PUBLISHED 09 December 2025
DOI 10.3389/fenvs.2025.1693898

Check for updates

OPEN ACCESS

EDITED BY
Paul V. Doskey,
Michigan Technological University,
United States

REVIEWED BY
Charuni Jayasekara,
The University of Melbourne, Australia
Michelle McKeown,
University College Cork, Ireland

*CORRESPONDENCE
Angela L. Creevy,
creevya@hope.ac.uk
Daniel Puppe,
daniel.puppe@zalf.de

RECEIVED 27 August 2025
REVISED 31 October 2025
ACCEPTED 07 November 2025
PUBLISHED 09 December 2025

CITATION
Creevy AL and Puppe D (2025) Microform matters: seasonal variations in peatland protozoic Si pools and the importance of microtopography.
Front. Environ. Sci. 13:1693898.
doi: 10.3389/fenvs.2025.1693898

COPYRIGHT
© 2025 Creevy and Puppe. This is an open-access article distributed under the terms of the Creative Commons Attribution License (CC BY). The use, distribution or reproduction in other forums is permitted, provided the original author(s) and the copyright owner(s) are credited and that the original publication in this journal is cited, in accordance with accepted academic practice. No use, distribution or reproduction is permitted which does not comply with these terms.

Microform matters: seasonal variations in peatland protozoic Si pools and the importance of microtopography

Angela L. Creevy[1]* and Daniel Puppe[2]*

[1]School of Computer Science and the Environment, Liverpool Hope University, Liverpool, United Kingdom, [2]Leibniz Centre for Agricultural Landscape Research (ZALF), Müncheberg, Germany

Healthy peatlands are the largest terrestrial carbon (C) store despite covering only approximately 3% of total global land surface. However, peatland health is threatened by anthropogenic exploitation and degradation by drainage. Consequently, large-scale ambitious projects to re-wet and restore peatlands have been initiated. It is hoped that they will sequester C and provide a nature-based solution to climate change. The organic-rich peat soils contained in peatlands play an important role in the global C cycle and other biogeochemical cycles, including global silicon (Si) cycling. Testate amoebae (TA) are a dominant group of microbial consumers in peatlands, and their siliceous shells form protozoic Si pools, which represent an important biological sink for Si in these ecosystems. Seasonal variations and the influence of peatland microtopography on protozoic Si pools are unexplored areas of research. In this study, we present data on protozoic Si pools in a former raised bog under restoration management. Our findings show variability in protozoic Si pools between seasons, microtopography, and vegetation cover. There was a clear trend of higher protozoic Si pools in hummocks than in hollows in all seasons, and higher protozoic Si pools were associated with higher water table depth and lower temperatures in colder/wetter months (November/autumn, February/winter) than that in warmer/drier months (May/spring, August/summer). These results suggest that future quantification of protozoic Si pools in peatlands should consider fine-scale spatiotemporal variables as an important feature in the experimental design.

KEYWORDS

peatland restoration, testate amoebae, spatiotemporal changes, protozoa, biogenic silica

Introduction

Peatlands are complex ecohydrological systems that deserve better understanding (Dise, 2009). They store a disproportionately large quantity of soil carbon (C) and it is crucial to better understand the impacts of land-use change on biogeochemical cycling. Globally, peatlands have been drained, often for agriculture and forestry, which accelerates decomposition and compromises their ability to act as a sink of atmospheric carbon dioxide (CO_2). Today, peatlands are recognized as providing a nature-based solution to climate change (Tanneberger et al., 2020). Large-scale, ambitious restoration projects are underway in temperate (Andersen et al., 2017) and tropical (Page et al., 2009) peatlands to try to restore the hydrology and reverse some of the damage. This is challenging given the

spatial heterogeneity of microtopography, which plays a significant role in various ecological, hydrologic, and biogeochemical processes (Rydin and Jeglum, 2013; Shukla et al., 2023) and is also influenced by human activity (Harris and Baird, 2019).

One of the strongest relationships with vegetational gradients in peatlands is the simple measure of the depth to the water table from the ground surface (Rydin and Jeglum, 2013). In this context, microtopography, i.e., small-scale spatial variations in peatland low points (hollows) and high points (hummocks), represents a key factor in peatland ecology (Graham et al., 2020). Vegetation composition and microtopography have been shown to have significant control on C fluxes from peatlands (Creevy et al., 2020; Perryman et al., 2022), but most land surface models fail to accurately represent peatland C emissions because they do not fully represent the hydrologic cycle or microtopography properly (Graham et al., 2022).

The accumulation of amorphous silica ($SiO_2 \cdot nH_2O$) formed by organisms (biogenic silica, BSi) created a biological loop that strongly controls silicon (Si) cycling in terrestrial ecosystems (see the reviews of Katz et al., 2021; Schaller et al., 2021 and references therein). Si fluxes from terrestrial ecosystems into the oceans then again control C cycling on a global scale because marine diatoms rely on Si bioavailability for reproduction, which then fixes large quantities of CO_2 via photosynthesis. Peatlands store large amounts of phytogenic Si, i.e., silica accumulated in plants, and the concentrations of dissolved Si in draining rivers in Sweden and Russia, for example, were found to be positively correlated with peat wetland coverage (Struyf and Conley, 2009). However, most studies investigating Si cycling in terrestrial environments focus on Si accumulation in plants (phytogenic Si), and our knowledge regarding other BSi pools is still scarce (Zaman et al., 2025). The ability to form siliceous structures (biosilicification) has evolved in various prokaryotes and eukaryotes, such as bacteria, fungi, protists, or sponges (Puppe, 2020).

One group of well-studied soil protists in peatland environments is testate amoebae (TA). Many TA taxa, almost all in the order Euglyphida, are characterized by siliceous shells made up of self-synthesized silica platelets, the so-called idiosomes. In terrestrial ecosystems, the accumulation of biogenic silica of protozoic origin results in the formation of corresponding protozoic Si pools (Sommer et al., 2013; Puppe et al., 2015; Creevy et al., 2016). As TA numbers can reach up to hundreds of thousands of individuals per gram in soils (Ehrmann et al., 2012), annual biosilicification by TA is equal to or even exceeds Si accumulation by trees in forest ecosystems (Puppe, 2020). TA are considered dominant microbial consumers in organic-rich peat soils (Wilkinson and Mitchell, 2010) and have been studied in terms of their bioindication value in peatlands undergoing restoration management in the United Kingdom (Swindles et al., 2016; Creevy et al., 2018; Evans et al., 2024). In *Sphagnum*-dominated peatlands, the number of TA taxa is naturally large, commonly exceeding the number of moss and vascular plant species (Mitchell et al., 2000a). More recently, protozoic Si pools have been shown to respond to peatland degradation and the loss of Si in peatland ecosystems caused by drainage for forestry and agriculture (anthropogenic desilication) (Qin et al., 2020; 2022) and restoration practices (Qin et al., 2021). However, despite advancing our understanding of the impacts of peatland degradation and restoration on Si cycling, we are still at the early stages of understanding the effects of peatland degradation and restoration on protozoic biosilicification (Qin et al., 2022).

In this study, we analyzed the spatiotemporal variations in protozoic Si pools in a former raised bog under restoration management. Our aim was to reveal the importance of time (seasonal variations) and microtopography (hummocks and hollows) for protozoic biosilicification in peatland, where trees have been cleared for restoration (termed forest clearance sites from herein, also referred to as forest-to-bog restoration). To do so, using a space-for-time substitution approach (Pickett, 1989), we examined TA assemblages and the corresponding protozoic Si pools in samples taken from hollows and hummocks at different dates (i.e., in August/summer, November/autumn, February/winter, and May/spring). We hypothesized (H1) that higher protozoic Si pools would be observed at the open and the oldest restoration area than at the youngest restoration area, where TA assemblages have been slower to recover due to the physical peat properties (Creevy et al., 2023). We expected (H2) that higher protozoic Si pools would be found in drier hummocks composed of ericaceous shrubs than in wetter hollows because root standing crop and production are greater in raised hummocks (Keiser et al., 2025). We further hypothesized (H3) that protozoic Si pools would be higher in May/spring and August/summer, in agreement with other seasonal studies (Heal, 1964), which have shown the maximum TA numbers in warmer growing seasons than in colder seasons. Our results on temporal (seasonal) and spatial (microtopographical) variations in protozoic Si pools will substantially deepen our understanding of Si cycling by TA in peatlands.

Methods

Study site and experimental design

The study was undertaken at Fenns, Whixall, and Bettisfield Moss National Nature Reserve, United Kingdom (52°92′24″ N, 2°76′94″ W). This lowland raised mire complex is situated in the counties of Shropshire and Wrexham at an altitude of 72 m above sea level. The monthly average air temperature ranges from 0.6 °C (minimum) to 21.0 °C (maximum), and the mean annual rainfall is 659.9 mm (average of 1981–2010 at the Shawbury Meteorological Station, located 22 km from the study site). Historically, the site was drained for commercial peat cutting during the 18th century, which ceased in 1990 (Leah et al., 1998). From ~1960s, areas around the site were planted with trees (lodgepole pine *Pinus contorta*, Norway spruce *Picea abies*, and Scots pine *Pinus sylvestris)* and managed for commercial forestry. Since the 1990s, restoration has involved damming drainage ditches to raise the water table, whole tree removal, scrub control, and brash removal. In areas of forest clearance (Figures 1a,b), the microtopography was in the form of equally spaced (usually 2 m) ridges and furrows and resembled the hummock–hollow microforms in areas not planted with trees.

At the first study site (RES17), trees were removed in 1998 (17 years prior to sampling) (n = 7); at the second study site (RES06), trees were removed in 2009 (6 years prior to sampling) (n = 7), and these sites were compared with an area not planted with trees (OPEN) (n = 7). OPEN study areas were not planted with trees and were not directly impacted by peat cutting. At RES06 (the

FIGURE 1
Satellite photographs (Google Earth) of the restoration sites in 2006 **(a)** and after large-scale tree removal in 2009 **(b)**. Representative vegetation composition of the study areas is shown below. Modified from Creevy et al. (2023).

youngest restoration area), ridges were dominated by *Calluna vulgaris* and bare peat/brash (n = 4), and furrows were dominated by *Eriophorum angustifolium* (n = 3). Ericaceous shrubs (*Vaccinium myrtillus*, *V. oxycoccos*, and *Erica tetralix*) and non-*Sphagnum* mosses (*Aulacomnium palustre* and *Pleurozium schreberi*) were dominant on ridges at RES17 (the oldest restoration area) and hummocks in OPEN study areas (n = 6). Hollows were dominated by *Sphagnum angustifolium* (n = 4) and *Eriophorum vaginatum*/*Sphagnum* (n = 4) (Figure 1).

The TA sampling campaign took place over 1 day in August/summer 2015 (n = 21), November/autumn 2015 (n = 21), February/winter 2016 (n = 21), and May/spring 2016 (n = 21) and encompassed hummocks/ridges (n = 40) and hollows/furrows (n = 44). The TA sampling approach followed Jassey et al. (2011) (and reference therein) in the collection of a composite sample from three permanently marked plots at each of the sample sites. The rationale for this approach was to avoid any bias due to spatial heterogeneity.

Environmental variables

The water table depth (WTD) and temperature were measured seasonally to correspond with TA sampling. WTD was measured using permanently installed dipwells located within 1 m of the TA sampling points, and the ambient temperature was measured using the Los Gatos Ultraportable Greenhouse Gas Analyzer (Model 915-0011). The following environmental variables were measured once during the study period in December 2015: pH, electrical conductivity, bulk organic matter content, moisture, and bulk density. For this, three replicate sub-samples were collected from each sampling point (n = 63) and prepared using standard methods (Chambers et al., 2010). pH and electrical conductivity were measured in the laboratory by mixing 20 mL of the surface sample with 25 mL of deionized water, and the samples were shaken at 400 rpm for 30 minutes and then centrifuged at 3,000 rpm for 5 minutes. A Hanna HI 98128 multi-parameter probe was used for measuring pH, and a Hanna HI 98311 probe was used for electrical conductivity. For bulk density, a 400-mL cylinder was used to carefully extract samples. Samples were weighed, oven-dried at 105 °C overnight, and reweighed to determine the bulk density (expressed in g cm^{-3}) and moisture content (in %); the methods were adapted from Chambers et al. (2010).

Testate amoebae preparation and quantification

Surface vegetation/peat samples (n = 84) of approximately 5 cm × 5 cm x 10 cm (250 cm^3) were collected from three permanently marked plots during a previous study (Creevy et al., 2023). To capture small-scale, i.e., microtopographical variation (hummocks vs. hollows), the experimental design allowed for

multiple sampling over time and the collection of a composite sample from each plot. The composite sample was the combination of three individual samples per plot, and all samples were frozen in the laboratory prior to preparation. Freezing the samples was favored over refrigeration to preserve the integrity of the specimens and slow metabolic activity. This was to allow an extended period (3 months) between the collection of samples and microscopic analysis. A modified version of Booth et al. (2010) was used to prepare TA samples. Samples were soaked and disaggregated in 50 mL of deionized water overnight and stirred occasionally. The sample was washed through a 250 µm sieve and centrifuged at 3,000 rpm for 3 minutes. Rose Bengal was added to distinguish living individuals. The number of TA was counted at ×400 magnification using a Prior Scientific Advanced Laboratory Microscope. In Creevy et al. (2023), the search effort was restricted to 100 individuals per sample, which is the standard in ecological and paleo-ecological studies (Payne and Mitchell, 2009). Morphological identification of TA was based on the guides of Charman et al. (2000), Ogden and Headley (1980), and Mazei and Tsyganov (2006).

Quantification of protozoic Si pools

Biosilicification of TA was quantified by multiplying the total number of individuals (living plus dead individuals) of a species (data from Creevy et al., 2023) with the corresponding species-specific silica content (Aoki et al., 2007). Subsequently, protozoic silica quantities were converted into protozoic Si quantities using a silica-to-Si conversion factor of 28/60 (SiO_2, M = 60.08 g mol^{-1}; Si, M = 28.085 g mol^{-1}) and summed up per sample (Puppe et al., 2014; 2018). As TA shell counts were restricted to 100 specimens (see subsection above), protozoic Si pools were finally calculated and expressed as nanogram (ng) of Si per 150 TA shells per sample to assure comparability to previous studies (Qin et al., 2021; 2022), which also had to deal with this restriction.

Statistical analysis

Differences in protozoic Si pools between hummocks and hollows were analyzed using an independent t-test, and an analysis of variance (ANOVA) was used to test for differences between the study areas (restoration age) and microtopography. Linear and monotonic relationships between WTD and protozoic Si pools were analyzed using Pearson's (r) and Spearman's rank (r_s) correlations (α level of 0.05), respectively. A multivariate ordination method, i.e., a cluster analysis (Ward's minimum variance method with squared Euclidean distances), was used to group the sampling sites based on (i) environmental variables (i.e., WTD, temperature, pH, electrical conductivity, bulk organic matter content, moisture, and bulk density) and (ii) TA abundances (in %). For the cluster analysis, the mean values for the different study areas (RES06, RES17, and OPEN) were calculated considering the sampling date (February/winter, May/spring, August/summer, and November/autumn) and microforms (hummocks and hollows). The mean protozoic Si pools in hummocks and hollows were calculated based on three (n = 3) or four (n = 4) field replicates (see subsection "Study site and experimental design"), which enabled a focus on differences between peat microforms (hummocks vs. hollows) rather than on the variability within a microform. This approach resulted in 24 "sites" (three study areas x four sampling dates x two microforms), which were used for cluster analysis. Environmental variables were standardized via Z-score transformation before clustering to standardize the data and exclude scale effects. A Kruskal–Wallis test was used to analyze the differences in temperature and WTD between the months/seasons. Statistical analyses were performed using IBM SPSS Statistics (versions 29 (ALC) and 22 (DP)).

Results

Environmental variables

WTD was significantly lower in August/summer than in other months/seasons (χ^2 (3) = 27.036, p = < 0.001). A similar trend was observed for ambient temperature, which was significantly higher in May/spring and August/summer (χ^2 (3) = 75.887, p = < 0.001). At RES06, WTD ranged from 2.8 to 56.2 cm (mean 28.3 cm), moisture content ranged from 71.4% to 81.8% (mean 75.1%), and pH ranged from 5.1 to 5.9 (mean 5.6) (Table 1). Electrical conductivity was the highest at OPEN (mean 18.4 µS cm^{-1}) and the lowest at RES17 (mean 13.5 µS cm^{-1}). Bulk organic matter was the lowest at RES06, ranging from 69.6% to 84.9% (mean 77.4%). At the oldest restoration site (RES17), WTD ranged from −5.6 cm to 38.4 cm (mean 12.6 cm), the moisture content ranged from 73.2% to 94.4% (mean 85.4%), and pH ranged from 5.1 to 5.5 (mean 5.2). The ambient temperature of the three study sites ranged from 11.2 °C (min) to 29.4 °C (max). Bulk organic matter was the highest at RES17, ranging from 85.3% to 98.4% (mean 93.3%). WTD at OPEN areas was lower than that in RES17 and ranged between 3.5 and 33.6 cm (mean 17.1 cm), with the bulk organic matter content ranging from 77.5% to 98.1% (mean 89.9%) and pH ranging from 4.8 to 5.2 (mean 5.0). In contrast, the moisture content was higher at OPEN areas, ranging from 83.7% to 93.7% (mean 88.6%) (Table 1).

In general, the cluster analysis based on environmental variables resulted in a distinct separation between the study areas RES06, RES17, and OPEN (Figure 2A). Two final clusters emerged: cluster 1 with the hummock and hollow sites of the study area OPEN and hollow sites of the study area RES17 and cluster 2 with hummock sites of the study area RES17 and the hummock and hollow sites of the study area RES06. These two clusters were joined with the highest linkage distance (i.e., 25), indicating the greatest dissimilarity between them. While in cluster 1 the hummock and hollow sites of the study area OPEN and the hollow sites of the study area RES17 were joined with relatively low linkage distances between 1 and 3, indicating great similarity, the differences between the sites in cluster 2 were slightly higher, with linkage distances between 1 and 6. The latter was found for the joining of the hummock sites of the study area RES17 and the hummock and hollow sites of the study area RES06.

Testate amoeba assemblages

A total of 54 TA taxa were identified in this study (Supplementary Table S1). The grouping of the sampling sites via

TABLE 1 Study area characteristics, geographic positions, and physico-chemical properties. The means and standard errors (SE) are provided. Significant differences between the study areas are reported (data from Creevy et al., 2023, except for ambient temperature).

Site name	Geographic position		Ambient temperature (°C)	pH	Conductivity (µS cm^{-1})	Bulk organic matter (%)	Moisture (%)	Bulk density (g cm^{-3})	WTD (cm)
	Latitude	Longitude	p >0.05	p <0.001	p = 0.007	p <0.001	p <0.001	p <0.001	p <0.001
RES06	52°93′52″	02°75′86″	22.1 (± 6.3)	5.6 (± 0.07)	14.6 (± 1.2)	77.4 (± 2.2)	75.1 (± 0.9)	0.10 (± 0.005)	28.3 (± 2.7)
RES17	52°93′49″	02°76′00″	20.3 (± 6.0)	5.2 (± 0.04)	13.5 (± 0.8)	93.3 (± 1.6)	85.4 (± 2.0)	0.06 (± 0.004)	12.6 (± 2.1)
OPEN	52°91′44″	02°77′23″	21.9 (± 5.3)	5.0 (± 0.06)	18.4 (± 1.3)	89.9 (± 2.4)	88.6 (± 1.1)	0.05 (± 0.003)	17.1 (± 1.6)

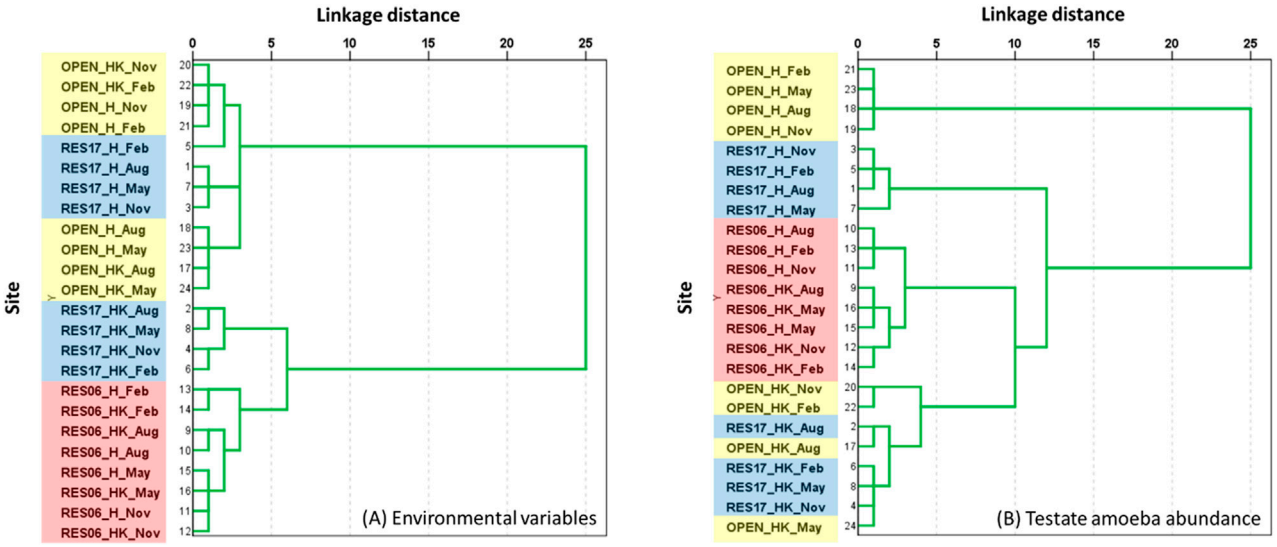

FIGURE 2
Dendrograms showing the grouping of the 24 sampling sites based on **(A)** environmental variables and **(B)** testate amoeba abundances (in %). The study areas are represented by different colors, i.e., yellow, OPEN; blue, RES17; and red, RES06. H, hollows; HK, hummocks; Aug, August/summer; Nov, November/autumn; Feb, February/winter; and May, May/spring.

cluster analysis based on TA abundances generally resulted in a distinct separation between the study areas RES06, RES17, and OPEN (Figure 2B). However, this grouping was not concurrent with the grouping of the sampling sites based on environmental variables (Figure 2). Based on TA abundances, two final clusters emerged: cluster 1 with the hollow sites of the study area OPEN and cluster 2 with all the remaining sites. Both clusters were joined with a relatively high linkage distance (i.e., 25), indicating the greatest dissimilarity. In cluster 1, the sites were joined with the lowest linkage distance (i.e., 1), indicating the greatest similarity among the sites included. Cluster 2 was subdivided into two further clusters, which were joined with a linkage distance of 12, indicating a relatively big dissimilarity between the sites included. While the first cluster comprised the hollow sites of study area RES17, the second cluster comprised the hollow and hummock sites of the study area RES06, the hummock sites of the study area OPEN, and the hummock sites of the study area RES17. This second cluster was again subdivided into two clusters, which were joined with a linkage distance of 10. The first cluster comprised the hollow and hummock sites of the study area RES06, and the second cluster comprised the hummock sites of the study areas OPEN and RES17.

The 24 sampling sites used for cluster analysis were characterized by site-specific TA assemblages, which differed in the occurrence (*cf.* Supplementary Table S1) and the abundance of TA taxa. In general, the three most abundant (top three) TA taxa represented ≥50% of the total TA record per site (except for sites RES06_HK_Aug and RES17_H_Aug; Table 2). The hollow and hummock sites of all study areas (i.e., RES06_H vs. RES06_HK, RES17_H vs. RES17_HK, and OPEN_H vs. OPEN_HK) showed clear differences regarding the top-three TA taxon occurrence and abundance. While the most common TA taxa at the hollow sites belonged to the order Arcellinida (*Nebela tincta*, *Hyalosphenia subflava*, and *Arcella discoides*) or the Stramenopiles (*Archerella flavum*), 50% of the most common TA taxa at hummock sites belonged to the order Euglyphida (*Trinema lineare*, *Corythion dubium*, and *Assulina muscorum*). The second most common TA taxa at the hollow sites showed a 4:8 Euglyphida: Arcellinida ratio, while at the hummock sites, the second most common TA taxa were

TABLE 2 Overview of the top three dominant TA taxa (in %) recorded at the 24 sampling sites used for cluster analysis.

Site	Most common		Second most common		Third most common		Proportion sum (%)
	Taxon	Proportion (%)	Taxon	Proportion (%)	Taxon	Proportion (%)	
RES06_H_Aug	*Nebela tincta*	30	*Trigonopyxis arcula*	12	*Corythion dubium*	**9**	50
RES06_H_Nov	*Nebela tincta*	34	*Trinema lineare*	**17**	*Trigonopyxis arcula*	15	66
RES06_H_Feb	*Nebela tincta*	31	*Trinema lineare*	**15**	*Corythion dubium*	**15**	62
RES06_H_May	*Hyalosphenia subflava*	22	*Nebela tincta*	18	*Trinema lineare*	**14**	54
RES06_HK_Aug	*Hyalosphenia subflava*	20	*Trigonopyxis arcula*	16	*Corythion dubium*	**11**	48
RES06_HK_Nov	*Trinema lineare*	**30**	*Trigonopyxis arcula*	25	*Nebela tincta*	14	68
RES06_HK_Feb	*Corythion dubium*	**24**	*Trinema lineare*	**21**	*Trigonopyxis arcula*	10	56
RES06_HK_May	*Trigonopyxis arcula*	28	*Hyalosphenia subflava*	17	*Trinema lineare*	**11**	55
RES17_H_Aug	*Arcella discoides*	18	*Cryptodifflugia oviformis*	17	*Nebela tincta*	10	46
RES17_H_Nov	*Arcella discoides*	24	*Nebela tincta*	17	*Cryptodifflugia oviformis*	11	52
RES17_H_Feb	*Arcella discoides*	21	*Corythion dubium*	**15**	*Nebela tincta*	14	50
RES17_H_May	*Arcella discoides*	48	***Euglypha strigosa***	**8**	*Corythion dubium*	**7**	63
RES17_HK_Aug	*Nebela tincta*	29	*Assulina muscorum*	**19**	*Trigonopyxis arcula*	13	61
RES17_HK_Nov	*Assulina muscorum*	**28**	*Corythion dubium*	**15**	*Nebela tincta*	15	58
RES17_HK_Feb	*Nebela tincta*	24	*Corythion dubium*	**21**	*Trinema lineare*	**10**	56
RES17_HK_May	*Nebela tincta*	29	*Corythion dubium*	**20**	*Assulina muscorum*	**17**	65
OPEN_H_Aug	*Archerella flavum*	52	*Nebela collaris*	13	*Assulina muscorum*	**7**	72
OPEN_H_Nov	*Archerella flavum*	39	*Cryptodifflugia oviformis*	16	*Nebela collaris*	10	65
OPEN_H_Feb	*Archerella flavum*	41	*Nebela collaris*	18	*Corythion dubium*	**6**	65
OPEN_H_May	*Archerella flavum*	42	*Nebela collaris*	19	*Hyalosphenia papilio*	8	69
OPEN_HK_Aug	*Nebela tincta*	42	*Assulina muscorum*	**27**	*Corythion dubium*	**14**	83
OPEN_HK_Nov	*Corythion dubium*	**36**	*Assulina muscorum*	**26**	*Nebela tincta*	11	73
OPEN_HK_Feb	*Corythion dubium*	**48**	*Assulina muscorum*	**17**	*Nebela tincta*	15	80
OPEN_HK_May	*Assulina muscorum*	**28**	*Nebela tincta*	24	*Corythion dubium*	**20**	72

H, hollows; HK, hummocks; Aug, August/summer; Nov, November/autumn; Feb, February/winter; May, May/spring. Euglyphida taxa and corresponding proportions are highlighted in bold to improve table readability.

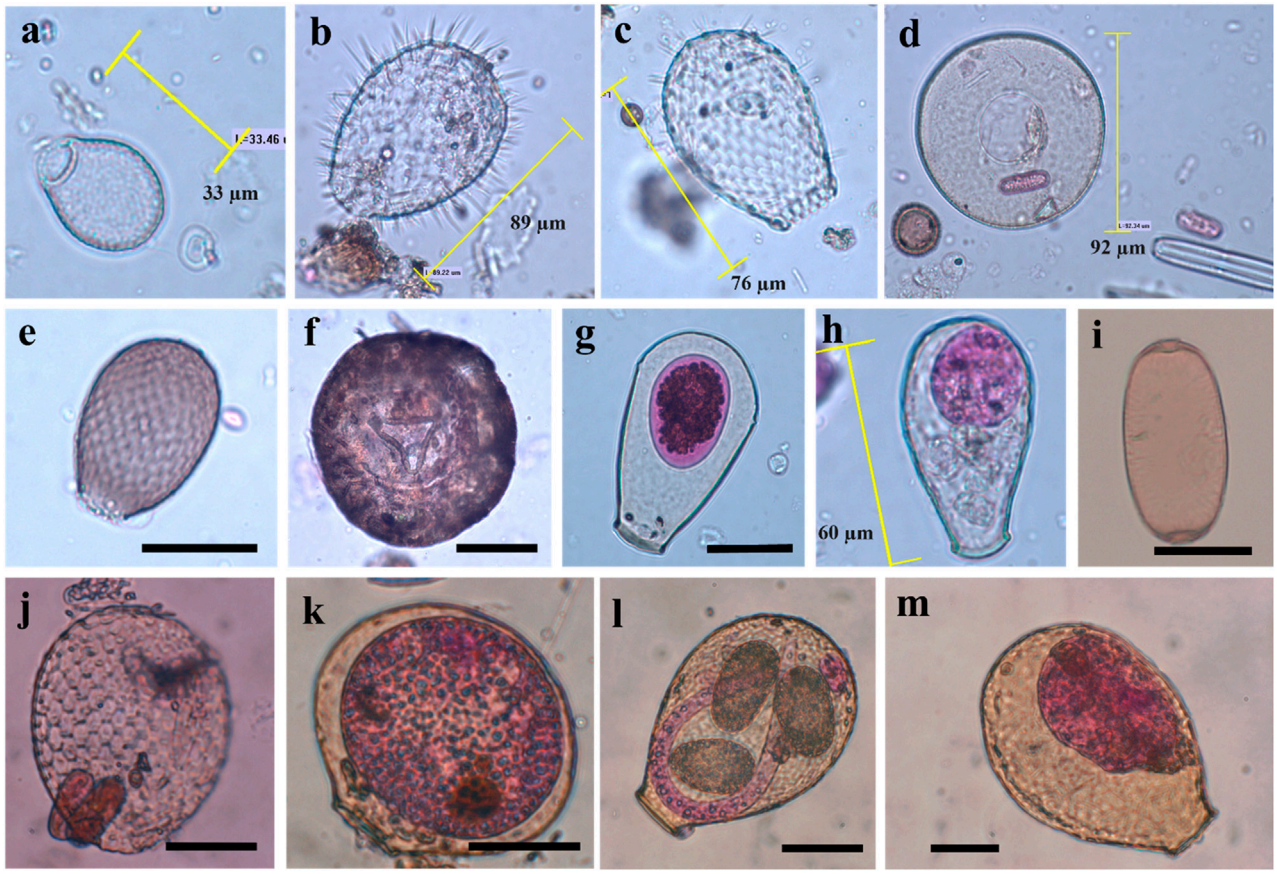

FIGURE 3
Representative images of some living **(g, h, k,** and **m)** and non-living **(a–f, i, j,** and **l)** TA found at the study areas: **(a)**. *Corythion dubium*, **(b)** *Placocista spinosa*, **(c)** *Euglypha strigosa*, **(d)** *Arcella (Galeripora) discoides*, **(e)** *Assulina muscorum*, **(f)** *Trigonopyxis arcula*, **(g)** *Hyalosphenia papilio*, **(h)** *Alabasta militaris*, **(i)** *Archerella flavum*, **(j)** *Assulina seminulum*, **(k)**. *Nebela flabellum*, **(l)** *N. tincta* major, and **(m)** *N. carinata*. Horizontal black scale bars represent 50 µm.

dominated by Euglyphida (eight taxa vs. four Arcellinida taxa). The third most common TA taxa at the hollow and hummock sites were represented by six Euglyphida and six Arcellinida taxa each. Moreover, TA taxon occurrence and abundance showed seasonal changes, which were characterized by switches in the order of the top-three TA taxa at a study site. Only at two sites (RES17_H and OPEN_H), we found no TA taxon switch during the season; i.e., one TA taxon was the most common one in all analyzed months (August/summer, November/autumn, February/winter, and May/spring): *A. discoides* for RES17_H and *A. flavum* for OPEN_H.

The proportion of living TA was 30.7% ± 16.5% in the hummocks and 30.7% ± 17.7% in the hollows, and the highest proportion of living taxa was found in August/summer (mean 36.2 ± 15.7), and the lowest was in May/spring (mean 25.9 ± 19.7). Representative images of some TA taxa (living and non-living) are shown (Figure 3). Euglyphida TA were the dominant taxa and accounted for a large proportion (40.6%) of all TA taxa observed. The dominant Euglyphida taxa in ascending order were as follows: *Corythion dubium* (1008 shells), *Assulina muscorum* (807), *T. lineare* (659), *Euglypha ciliata* (258), *Euglypha rotunda laevis* type (203), *Euglypha* spp. (151), *Euglypha strigosa* (128), *Euglypha compressa* (115), *Trinema enchelys* (64), and *Trinema complanatum* (4) (Table 3).

Protozoic Si pools

Protozoic Si pools were variable between the three study areas and ranged from a minimum of 3.4 to a maximum of 93.8 ng per 150 shells. The mean protozoic Si pool was higher at RES17 (45.5 ± 3.4) than at RES06 (34.3 ± 2.9), with greater dispersion in OPEN areas not planted with trees (mean 37.1 ± 5.3). The timing of plantation removal had no significant effect on protozoic Si pools, and there was no significant difference in protozoic Si pools between the three treatments/study areas ($F(2, 80) = 2.220$, $p = 0.115$) (Figure 4).

In contrast with the study area, vegetation showed significant variation in protozoic Si pools. Ericaceous shrubs on hummocks supported a large proportion (42.1%) of the protozoic Si pool, and protozoic Si pools in ericaceous shrubs were significantly greater than those in other vegetation types ($F(4, 79) = 9.742$, $p < 0.001$) (Figure 5).

Along with the vegetation type, microtopography also showed significant variation in protozoic Si pools ranging from 3.4 to 93.8 ng per 150 shells. The mean protozoic Si pool was significantly higher in hummocks (49.0 ± 3.3) than in hollows (29.5 ± 2.5) ($t_{1,82} = -4.759$, $p < 0.001$) (Figure 6).

Across all seasons, there was a general trend of lower protozoic Si pools in hollows than in hummocks, and collectively, there was a

TABLE 3 Overview of the proportion of Euglyphida TA taxa (in %) recorded at the 24 sampling sites used for cluster analysis.

Site	Taxon proportion (%)													Sum (%)
	A. mus	*A. sem*	*C. dub*	*T. pul*	*E. cil*	*E. com*	*E. rot*	*E. str*	*E. tub*	*P. spi*	*T. com*	*T. enc*	*T. lin*	
RES06_H_Aug	8	0	9	2	4	0	3	0	3	0	0	0	6	**37**
RES06_H_Nov	4	0	2	0	0	0	5	0	1	0	0	2	**17**	**30**
RES06_H_Feb	5	0	**15**	0	5	0	4	0	5	0	0	1	**15**	**51**
RES06_H_May	3	0	8	0	4	0	6	0	2	0	0	0	**14**	**37**
RES06_HK_Aug	6	0	**11**	1	3	0	4	0	4	0	0	0	**11**	**39**
RES06_HK_Nov	6	0	5	0	0	0	3	0	1	0	0	1	**30**	**45**
RES06_HK_Feb	4	0	**24**	1	6	0	4	0	5	0	0	1	**21**	**66**
RES06_HK_May	6	0	7	0	0	0	4	0	7	0	0	0	**11**	**36**
RES17_H_Aug	6	0	8	0	7	3	0	8	2	0	0	0	1	**36**
RES17_H_Nov	9	0	9	0	2	5	5	1	3	0	0	0	1	**35**
RES17_H_Feb	5	0	**15**	0	2	**12**	1	2	0	0	0	0	5	**43**
RES17_H_May	4	0	7	2	4	4	1	8	0	0	0	0	1	**32**
RES17_HK_Aug	**19**	1	5	0	1	2	4	3	0	0	0	2	2	**39**
RES17_HK_Nov	**28**	6	**15**	0	2	0	1	0	2	0	0	0	9	**64**
RES17_HK_Feb	7	3	**21**	4	4	0	1	0	3	0	0	2	**10**	**57**
RES17_HK_May	**17**	1	**20**	3	3	0	1	5	0	0	0	0	8	**57**
OPEN_H_Aug	7	0	0	0	3	0	0	1	0	0	0	0	2	**14**
OPEN_H_Nov	7	0	1	0	4	1	1	0	0	0	0	0	1	**16**
OPEN_H_Feb	5	0	6	0	5	2	2	0	1	0	0	1	3	**26**
OPEN_H_May	2	0	5	0	2	0	1	3	0	0	0	0	2	**16**
OPEN_HK_Aug	**27**	0	**14**	0	0	0	1	0	0	0	0	3	1	**46**
OPEN_HK_Nov	**26**	1	**36**	0	0	0	8	0	2	0	0	1	4	**78**
OPEN_HK_Feb	**17**	0	**48**	0	9	0	2	0	0	0	0	2	2	**81**
OPEN_HK_May	**28**	0	**20**	0	2	0	3	0	0	0	0	2	6	**60**

A. mus, *Assulina muscorum*; A. sem, *Assulina seminulum*; C. dub, *Corythion dubium*; T. pul, *Trachelocorythion pulchellum* (recorded as *Corythion pulchellum*); E. cil, *Euglypha ciliata*; E. com, *Euglypha compressa*; E. rot, *Euglypha rotunda laevis*; E. str, *Euglypha strigosa*; E. tub, *Euglypha tuberculata*; P. spi, *Placocista spinosa*; T. com, *Trinema complanatum*; T. enc, *Trinema enchelys*; T. lin, *Trinema lineare*; H, hollows; HK, hummocks; Aug, August/summer; Nov, November/autumn; Feb, February/winter, and May, May/spring. Two-digit numbers (≥10) are highlighted in bold to improve table readability.

statistically significant difference in seasonal protozoic Si pools between microforms (F (7, 76) = 4.660, p = <0.001) (Figure 6). Seasonal protozoic Si pools at hummocks did not differ significantly (F (3, 36) = 1.572, p = 0.213) but were notably higher in November/autumn (49.5 ± 6.3) and February/winter (59.4 ± 5.7) than in August/summer (39.8 ± 5.8) and May/spring (47.1 ± 7.8) and corresponded with higher WTD (i.e., wetter conditions). In hollows, seasonal protozoic Si pools did not differ significantly (F (3, 40) = 1.394, p = 0.259) but, similar to hummocks, were the highest in February/winter (35.9 ± 5.8). While there was a significant negative correlation observed between protozoic Si pools and WTD in hummocks (r = −0.449, p = 0.004; r_s = −0.541, p < 0.001; n = 40), there was no significant relationship between the protozoic Si pool and WTD in hollows (r = −0.091, p = 0.559; r_s = −0.117, p = 0.451; n = 44). The mean proportion of living TA in hummocks ranged between 26% (February/winter) and 34% (August/summer). In hollows, the range between the minimal and maximal mean proportion of living TA was higher, with 21% in May/spring and 39% in August/summer (Figure 6).

Discussion

Impacts of land-use change and restoration on protozoic Si pools

The results here demonstrate how land-use change and restoration influence peatland protozoic Si pools. We rejected the

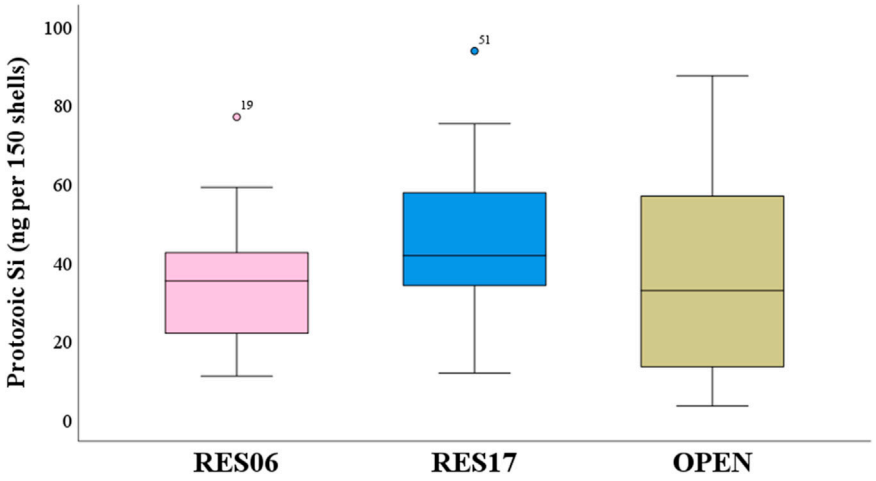

FIGURE 4
Differences in protozoic Si pools between the three study areas. The top, middle, and bottom boxplot line represent the 75th, 50th, and 25th percentiles, and the horizontal lines represent the 10th and 90th percentiles. Numbered circles represent outliers.

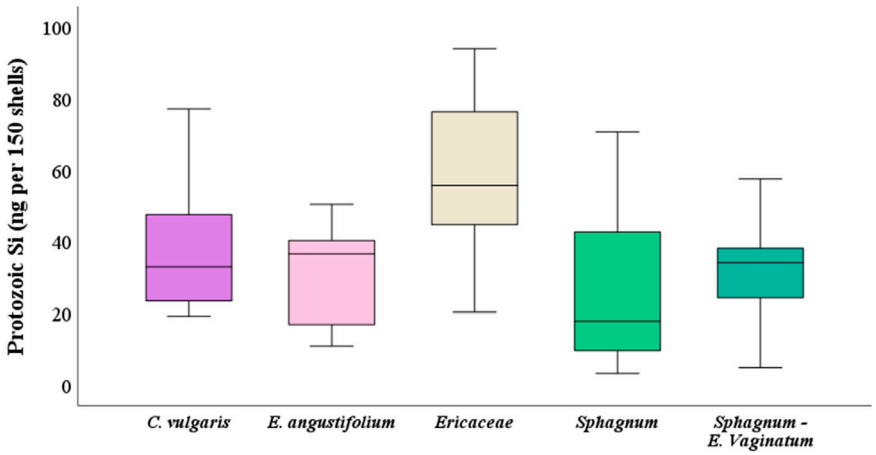

FIGURE 5
Variation in protozoic Si pools between different vegetation types. The top, middle, and bottom boxplot line represent the 75th, 50th, and 25th percentiles, and the horizontal lines represent the 10th and 90th percentiles.

hypothesis H1 that higher protozoic Si pools would be observed at the open and oldest restoration area compared with that at the youngest restoration area as we found no significant differences in protozoic Si pools between restoration ages. Possible explanations include legacy effects from forestry, such as nutrient input from fertilization and the persistence of ridge–furrow microtopography, which may override age differences. Additionally, this could be attributed to differences in vegetation recovery speed between sites, particularly with ericaceous shrubs and *Sphagnum* species. It is recognized that the space-for-time substitution approach used in this study, while legitimate, does carry assumptions—for example, that restoration sites follow similar trajectories. There is some evidence to show that this is not the case because local physicochemical peat properties are an important driver of TA assemblages at forest-clearance peatland restoration sites (Creevy et al., 2023). It is also worth noting that while the OPEN (control) study area was left untouched by peat cutting and was not planted with trees, this area may have been indirectly affected by the extensive drainage system on this degraded raised bog.

While deforestation generally has been shown to lead to increased riverine Si transport from terrestrial to aquatic ecosystems in the short term (years to decades), the long-term (>250 years) cultivation of formerly forested areas has decreased this transport due to anthropogenic Si exports via crop harvesting in combination with higher soil erosion rates (Conley et al., 2008; Struyf et al., 2010a). On a global scale, terrestrial ecosystems, including peatlands, control the export of dissolved silica from continents to the oceans, whereby large proportions (i.e., approximately 30%–90%) of these fluxes are linked to terrestrial BSi pools (Struyf and Conley, 2012). However, while the role of vegetation and corresponding phytogenic Si pools for Si cycling in peatland environments has been recognized

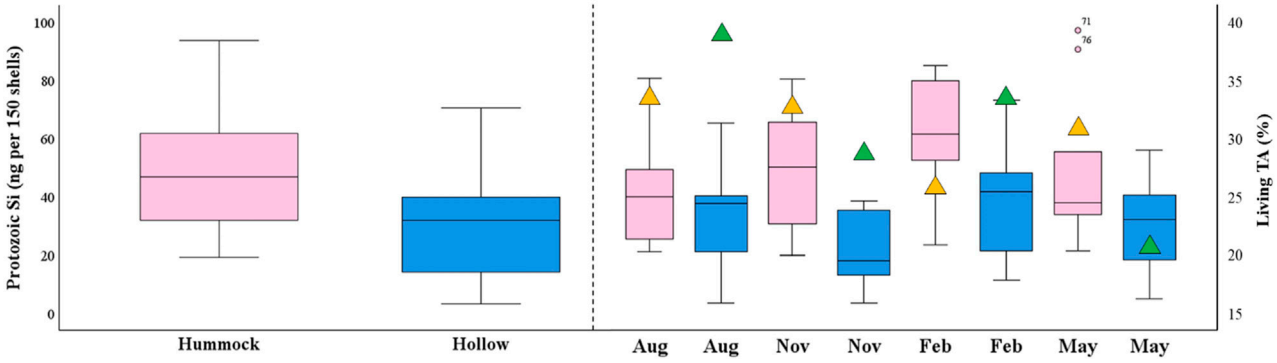

FIGURE 6
Variation in protozoic Si pools in hollows (n = 44) and hummocks (n = 40) and seasonal variations. The top, middle, and bottom boxplot line represent the 75th, 50th, and 25th percentiles, and the horizontal lines represent the 10th and 90th percentiles. Numbered circles represent outliers. Orange and green triangles indicate the mean proportion of living TA in the hummocks and hollows, respectively.

(Struyf and Conley, 2009), the potential importance of protozoic Si pools is sparsely documented. We are only aware of three other studies that have quantified protozoic Si pools in peatlands (Qin et al., 2020; Qin et al., 2021; Qin et al., 2022).

These studies showed that (i) soil moisture is a key control of protozoic Si pool quantity, which significantly differed between intact peatland and cropland, i.e., former peatland that was drained for agriculture (Qin et al., 2020), and (ii) the protozoic Si pool quantity is not necessarily linked to a rich TA biodiversity as protozoic Si pools were negatively correlated with TA taxon richness and diversity (Qin et al., 2021). The latter was corroborated on a continental scale by Qin et al. (2022), who found a decline in TA biodiversity in Asian peatlands caused by anthropogenic peatland degradation to be accompanied by an unexpected increase in protozoic biosilicification. In our study, over 40% of the overall TA assemblage consisted of members of the order Euglyphida. These taxa produce self-secreted (autogenous) siliceous platelets (idiosomes) (Ogden and Headley, 1980), which is why they have been routinely—and exclusively—used for protozoic Si pool quantification (Puppe, 2020). As a few taxa (i.e., *Lesquereusia*, *Netzelia*, and *Quadrulella*) with autogenous siliceous shells can also be found in the order Arcellinida, the protozoic Si pools reported in the literature so far could be underestimated (see discussion in Puppe, 2020). However, as we did not record specimens of these Arcellinida TA taxa at all, this aspect is negligible in our study.

Degraded peatlands are often the focus of ecological restoration, and large-scale restoration projects are underway (Andersen et al., 2017; Bonn et al., 2016). This is the first study to quantify protozoic biosilicification in peatland where trees have been cleared for restoration. We observed that younger (<10 years) restoration areas had lower protozoic Si pools than older (>15 years) restoration areas. This is in line with the findings of Puppe et al. (2014), who showed that the protozoic Si pool is built up rapidly in the very young (3-, 5-, and 10-year-old) initial ecosystem states of an artificial catchment and is strongly linked to plant growth. On the contrary, Qin et al. (2021) found no statistically significant differences between protozoic Si pool sizes in differently aged (5-months, 1-year, and 2-year-old) *Sphagnum*-growing plots. Generally, these differences can be mainly ascribed to two factors: (i) the environmental conditions (e.g., moisture, pH, or nutrient availability) of the (new) habitat and (ii) the period of time that is considered, i.e., the time available for TA population development. Naturally, both factors are inextricably linked to each other, and thus, they control the immigration and colonization success of TA at these habitats (*cf.* Wanner et al., 2008).

While Qin et al. (2021) considered a relatively short period of time (i.e., 19 months) in their analysis of *Sphagnum*-growing plots, the period considered by Puppe et al. (2014) was comparably longer (7 years). This difference was directly reflected in the results: while Qin et al. (2021) found no differences in pH and WTD between the analyzed *Sphagnum*-growing plots, Puppe et al. (2014) found substantial changes in soil pH between the analyzed plots. Furthermore, the existing TA assemblages at the start of the experiment can be considered largely different (*Sphagnum* vs. sandy substrate). While the youngest (5-month- old) *Sphagnum*-growing plots in the study of Qin et al. (2021) already showed a relatively high TA taxon richness, the youngest (3-year-old) sandy substrate plots analyzed by Puppe et al. (2014) were quite poor in TA, which predominantly arrived at this newly exposed area by air (*cf.* Wanner et al., 2015). In our study, the WTD substantially differed between the analyzed study areas, which was directly reflected in the composition of the corresponding TA assemblages. Moreover, at forest clearance sites nutrients can leach from felling brash, and this higher fertility might slow restoration at these sites (Hancock et al., 2018 and references therein) and affect TA assemblages. TA are known to quickly respond to small changes in hydrological conditions and nutrient availability, which is why they are widely used as bio-indicators in peatland hummocks and hollows (Creevy et al., 2018; Evans et al., 2025).

Importance of microtopography

While land-use change has been shown previously to have a significant impact on protozoic Si pools (Qin et al., 2020; 2022), microtopography has not been explored. In the present study, we

accepted the hypothesis H2 that higher protozoic Si pools would be found in drier hummocks composed of ericaceous shrubs than in wetter hollows. We speculate that this is the result of root standing crop and production, which are greater in raised hummocks (Keiser et al., 2025). The scale is an important factor in empirical peatland research (Limpens et al., 2008), and this is also true of the quantification of protozoic Si pools. Our findings support the claim that biogenic Si pools are variable in wetland environments (Struyf and Conley, 2009). As wetlands represent a link between terrestrial and aquatic ecosystems, they are important for biogeochemical Si cycling at the landscape scale, which is reflected in large BSi (i.e., phytolith and diatom frustule) pools with relatively large ranges (Struyf et al., 2010b). Such variability in the BSi pool size was also recorded for protozoic Si pools. For example, Creevy et al. (2016) found protozoic Si pools in different habitats within the Mere Sands Wood nature reserve in NW England to range between 5 and 82 ng Si g^{-1} sample dry mass. At the peatland microform level, we show that small-scale variations with higher protozoic Si pools are found in hummocks compared with hollows. These findings have important implications for forest clearance at peatland restoration sites because the artificial ridge–furrow topography persists for many years after the trees are removed.

For the first time, this study shows how restoration impacts protozoic biosilicification in peatlands at the microform level. Peatland microtopography has profound effects on hydrology, temperature, light availability, nutrient cycling, and peat accumulation (Rydin and Jeglum, 2013), but, despite this, there are no other studies that have quantified protozoic Si pools in hummock and hollow microforms. In the present study, the protozoic Si pool was the highest in shrubs on hummocks compared with other studied vegetation types, and at the youngest restoration area, hummocks were composed of *C. vulgaris* and bare peat and brash. Vegetation establishment was slow at the youngest restoration area in comparison with the oldest restoration area which was dominated by dense ericaceous shrubs and non-*Sphagnum* mosses and more closely resembled open conditions. Studies at comparable sites have shown that vegetation on steeper ridges often show the poorest vegetation recovery (Hancock et al., 2018). Collectively, in this study, protozoic Si pools were the highest in ericaceous shrubs on hummocks at unforested sites and ridges at restoration sites.

In general, the (horizontal and vertical) spatial variability of TA assemblages is quite large in bog microforms (Mitchell et al., 2000b; Jassey et al., 2011; Lizoňová et al., 2019). In our study, there was a clear separation of TA taxa abundances between restoration areas, with greater abundance of xerophilous taxa occurring in hummock microforms and increased proportions of hygrophilous taxa in hollow microsites. Roe et al. (2017) investigated TA communities in the hummock–hollow transition and found considerable variability, especially in the uppermost acrotelmic peat layers. In their study, they found that hollows were characterized by a combination of xerophilous/hygrophilous taxa. They report that spined forms of the TA genus *Euglypha* (e.g., *E. strigosa*) were abundant in the upper 10 cm. In this study, we found that *E. strigosa* tended to be found in wetter hollows, and this taxon, along with *Galeripora discoides* and *Nebela carinata*, was most abundant at the oldest restoration area, where WTD was the highest and most variable. Sullivan and Booth (2011) showed that short-term environmental variability was often higher at hollows than at hummocks. In the present study, the proportion of living TA was more variable in hummocks, between 5% and 62%, but on average, the proportion of living individuals was similar in hummocks and hollows. These findings differ from those of Mazei and Tsyganov (2007), who found the maximum live abundances of TA in dry habitats, such as hummocks.

As the spatial distribution of TA and the proportion of living TA control the protozoic Si pool size and biosilicification rates, respectively, further studies should quantify protozoic Si pools along the vegetation gradients at peatland restoration sites. In this context, spatial heterogeneities in Si pool sizes should be considered to reduce inaccuracies (caused by the large Si pool size ranges) in quantifications of Si pools on the landscape/ecosystem scale, which are also known from aboveground phytogenic Si pools (Wehrhan et al., 2021). In addition, we recognize that intra- and interspecific variability in silica content was not captured in our study. This knowledge is crucial to reliably evaluate the importance of TA for Si cycling in (global) budget studies. Due to their large abundances in peatlands, TA might play a role comparable to that of diatoms in these ecosystems (*cf.*, Kokfelt et al., 2010).

Temporal dynamics and protozoic Si pools

Generally, Aoki et al. (2007) were the first to quantify protozoic biosilicification in terrestrial ecosystems. For a pine–oak (*Pinus densiflora* and *Quercus variabilis*) forest soil in Japan, these authors reported protozoic silica pool quantities in different months (i.e., April, November, and December) ranging between 0.45 kg SiO_2 ha^{-2} (December) and 1.57 kg SiO_2 ha^{-2} (April) (max/min ratio: 3.5). Compared to the results of Aoki et al. (2007), we found peatland protozoic Si pools to exhibit a higher seasonal variability, with ranges between 3.4 (August/summer) and 70.6 (February/winter) ng Si per 150 shells (max./min ratio: 20.8) and 19.3 (November/autumn) and 93.8 (May/spring) ng Si per 150 shells (max./min ratio: 4.9) in hollows and hummocks, respectively. Based on our findings, we suggest future studies should consider spatiotemporal TA heterogeneities in protozoic Si pool quantification at the landscape/ecosystem scale. Such seasonal variations are already well-documented in other Si-accumulating protists, i.e., marine and freshwater diatoms (Ragueneau et al., 1994; Hughes et al., 2011), and have also been reported for Si cycling in terrestrial plant–soil systems (Gérard et al., 2008; Zhou et al., 2025). While diatom reproduction is controlled by the concentration of bioavailable Si (monomeric silicic acid) in open waters (Tréguer and De La Rocha, 2013), a relationship between bioavailable Si in the soil solution and TA in forest soils (Puppe et al., 2015) or peatlands (Qin et al., 2020) has not been observed yet.

Although our results are limited to sampling over 4 months, they demonstrated some clear patterns. Surprisingly, in hummocks, protozoic Si pools were higher in colder and wetter months (November/autumn and February/winter) than in warmer/drier months (August/summer and May/spring). We, therefore, rejected the hypothesis H3 that protozoic Si pools would be higher in May/spring and August/summer. Heal (1964) observed

the maximum numbers of TA during the May-to-October period, with lower total numbers in fall when the organisms encysted for the winter. Other studies have demonstrated seasonal changes in TA composition in *Sphagnum* peatlands (Warner et al., 2007; Marcisz et al., 2014), but they sampled from only May to October, and few studies have quantified TA during winter (Mazei and Tsyganov, 2007). We agree with Sullivan and Booth (2011) that typical sampling procedures for TA integrate several years of test accumulation as living, non-living, and encysted tests. In the present study, a higher proportion of living individuals was found in August/summer and was probably a function of substrate moisture (Mazei et al., 2020). However, this peak in the number of living individuals did not correspond with higher protozoic Si pools. As knowledge of seasonal dynamics in protozoic Si pools is lacking, our results provide a starting point for further studies of this aspect in the future.

Si is an important element in peatlands (Rydin and Jeglum, 2013), and these ecosystems store large amounts of well-studied phytogenic silica that enters the organic soil in plant litter. Si is subsequently cycled from this plant litter as dissolved silica and is taken up by plants in the form of monomeric silicic acid (H_4SiO_4) (Struyf and Conley, 2012). Wetlands are known hotspots for both nitrogen and phosphorus cycling (Struyf and Conley, 2009), and the supply of nutrients such as nitrogen, phosphorus, potassium, and calcium results in increases in the relative biomasses of Bacillariophyceae (diatoms) and a decrease in the relative proportion of TA (Gilbert et al., 1998). Bacillariophyceae (diatoms) biomineralize silica and reach peak biomass in the period from the end of July to the end of August. Studies demonstrate that microbial communities and their functions are in a rapid state of change throughout the year, constantly adapting to variations in inputs to the system (for example, fresh organic matter) and altering the course of subsequent element cycling (Andersen et al., 2013). At forest clearance sites, we suggest that a combination of modifications in aboveground vegetation, the addition of fertilizers, and seasonal changes in litter condition might result in profound changes in the protozoic Si pool. Future high-resolution studies accounting for the feedback between WTD, plant root exudates, season (i.e., plant senescence), and protozoic Si pools are needed to capture these small-scale variations to better understand the impacts of peatland degradation and restoration on protozoic biosilicification.

Directions for future research

Protozoic Si pools are a largely unexplored area of research, and this is especially true at peatland restoration sites. The ecological and biogeochemical implications of peatland restoration on protozoic Si pools require further research because small-scale variations in protozoic Si pools between microforms are likely to impact ecosystem Si budgets on a large-scale. In this study, we show the potential of TA to create hotspots of Si at the microform level and highlight the potential of protozoic Si pools to be used as a proxy to monitor the trajectory of peatland restoration. Peatland restoration (ultimately, hydrological restoration) aims to raise the water table to create favorable conditions for peat-forming vegetation. The correlation between WTD and protozoic Si pools in hummocks requires further studies to determine the drivers. For instance, is this pattern the result of differential oxygen and nutrient availability at different WTDs, and/or are ericaceous shrubs providing litter and root exudates that influence microbial activity?

Based on the results of our study, it is unclear whether protozoic Si pools are controlled more by TA activity or by the preservation and turnover of TA shells. Previous studies showed that protozoic Si pools are mainly represented by dead (accumulated) TA shells (Sommer et al., 2013; Puppe et al., 2015; this study). However, biosilicification rates by living TA are equal to or even exceed the Si uptake by trees (Puppe, 2020). The preservation of TA shells in forest soils is assumed to be quite low—i.e., euglyphid shells have been found to decompose relatively fast (Lousier and Parkinson, 1981). However, no data on TA shell decomposition in peatlands are available (*cf.* Mitchell et al., 2008). Moreover, there is no information on the dissolution of idiosomes (the silica platelets that are used for shell construction), which might be quite abundant in soil (Puppe et al., 2022).

We found a negligible difference in the proportions of living and non-living individuals between hummocks and hollows, and the proportions of living individuals were the highest in August (and corresponded with the growing season) and the lowest in May, which reflects test accumulation. We do, however, acknowledge that a yearly seasonal sampling regime does not capture inter-annual variation. Restoration age was expected to influence protozoic Si accumulation due to vegetation succession (Creevy et al., 2023). Interestingly, there is some evidence to suggest that diatoms may thrive in the transition from one peatland vegetation type to another (Kokfelt et al., 2009). To start addressing this knowledge gap, future long-term, inter-annual studies should focus on quantifying living protozoic Si pools alongside silica-producing diatoms, which also exhibit seasonal cycles. Moreover, future studies quantifying protozoic Si pools in peatlands should consider spatial (microtopography) heterogeneities. This is crucial for a more precise quantification of protozoic Si pools on a landscape/ecosystem scale. Quantitative models based on these data might be further used for the paleoecological reconstruction of the past biosilicification rates of TA in peatlands.

Data availability statement

The original contributions presented in the study are included in the article/Supplementary Material; further inquiries can be directed to the corresponding authors.

Author contributions

AC: Conceptualization, Data curation, Formal analysis, Validation, Visualization, Writing – original draft, Writing – review and editing, Investigation. DP: Conceptualization, Data curation, Formal analysis, Validation, Visualization, Writing – original draft, Writing – review and editing.

Funding

The authors declare that financial support was received for the research and/or publication of this article. Data collection for this

work was funded by a Graduate Teaching/PhD Scholarship to AC from Edge Hill University, United Kingdom.

Acknowledgements

The authors greatly appreciate Joan Daniels M.B.E. and Peter Bowyer from Natural England and Edward Wardle for providing access to the study areas and for sharing the local knowledge of the study site.

Conflict of interest

The authors declare that the research was conducted in the absence of any commercial or financial relationships that could be construed as a potential conflict of interest.

Generative AI statement

The authors declare that no Generative AI was used in the creation of this manuscript.

Any alternative text (alt text) provided alongside figures in this article has been generated by Frontiers with the support of artificial intelligence and reasonable efforts have been made to ensure accuracy, including review by the authors wherever possible. If you identify any issues, please contact us.

Publisher's note

All claims expressed in this article are solely those of the authors and do not necessarily represent those of their affiliated organizations, or those of the publisher, the editors and the reviewers. Any product that may be evaluated in this article, or claim that may be made by its manufacturer, is not guaranteed or endorsed by the publisher.

Supplementary material

The Supplementary Material for this article can be found online at: https://www.frontiersin.org/articles/10.3389/fenvs.2025.1693898/full#supplementary-material

References

Andersen, R., Chapman, S. J., and Artz, R. R. E. (2013). Microbial communities in natural and disturbed peatlands: a review. *Soil Biol. Biochem.* 57, 979–994. doi:10.1016/j.soilbio.2012.10.003

Andersen, R., Farrell, C., Graf, M., Muller, F., Calvar, E., Frankard, P., et al. (2017). An overview of the progress and challenges of peatland restoration in Western Europe. *Restor. Ecol.* 25 (2), 271–282. doi:10.1111/rec.12415

Aoki, Y., Hoshino, M., and Matsubara, T. (2007). Silica and testate amoebae in a soil under pine–oak forest. *Geoderma* 142 (1-2), 29–35. doi:10.1016/j.geoderma.2007.07.009

Bonn, A., Allott, T., Evans, M., Joosten, H., and Stoneman, R. (2016). *Peatland restoration and ecosystem services: science, policy and practice.* Cambridge University Press.

Booth, R. K., Lamentowicz, M., and Charman, D. J. (2010). Preparation and analysis of testate amoebae in peatland palaeoenvironmental studies. *Mires Peat* 7, 1–7. doi:10.19189/001c.128409

Chambers, F. M., Beilman, D. W., and Yu, Z. (2010). Methods for determining peat humification and for quantifying peat bulk density, organic matter and carbon content for palaeostudies of climate and peatland carbon dynamics. *Mires Peat* 7, 1–10. doi:10.19189/001c.128415

Charman, D. J., Hendon, D., and Woodland, W. A. (2000). *The identification of testate amoebae in peats*, 9. London: Quaternary Research Association Technical Guide.

Conley, D. J., Likens, G. E., Buso, D. C., Saccone, L., Bailey, S. W., and Johnson, C. E. (2008). Deforestation causes increased dissolved silicate losses in the hubbard brook experimental forest. *Glob. Change Biol.* 14 (11), 2548–2554. doi:10.1111/j.1365-2486.2008.01667.x

Creevy, A. L., Fisher, J., Puppe, D., and Wilkinson, D. M. (2016). Protist diversity on a nature reserve in NW England–with particular reference to their role in soil biogenic silicon pools. *Pedobiologia* 59 (1–2), 51–59. doi:10.1016/j.pedobi.2016.02.001

Creevy, A. L., Andersen, R., Rowson, J. G., and Payne, R. J. (2018). Testate amoebae as functionally significant bioindicators in forest-to-bog restoration. *Ecol. Indic.* 84, 274–282. doi:10.1016/j.ecolind.2017.08.062

Creevy, A. L., Payne, R. J., Andersen, R., and Rowson, J. G. (2020). Annual gaseous carbon budgets of forest-to-bog restoration sites are strongly determined by vegetation composition. *Sci. Total Environ.* 705, 135863. doi:10.1016/j.scitotenv.2019.135863

Creevy, A. L., Wilkinson, D. M., Andersen, R., and Payne, R. J. (2023). Testate amoebae response and vegetation composition after plantation removal on a former raised bog. *Eur. J. Protistology* 89, 125977. doi:10.1016/j.ejop.2023.125977

Dise, N. B. (2009). Peatland response to global change. *Science* 326, 810–811. doi:10.1126/science.1174268

Ehrmann, O., Puppe, D., Wanner, M., Kaczorek, D., and Sommer, M. (2012). Testate amoebae in 31 mature forest ecosystems–densities and micro-distribution in soils. *Eur. Journal Protistology* 48 (3), 161–168. doi:10.1016/j.ejop.2012.01.003

Evans, C. R., Mullan, D. J., Roe, H. M., Fox, P. M., Gray, S., and Swindles, G. T. (2024). Response of testate amoeba assemblages to peatland drain blocking. *Wetl. Ecol. Manag.* 32 (1), 1–18. doi:10.1007/s11273-023-09949-w

Evans, C. R., Hatton, D. A., and Swindles, G. T. (2025). Testate Amoebae are informative bioindicators of critically high ammonia deposition on peatlands. *Eur. J. Protistology* 99, 126147. doi:10.1016/j.ejop.2025.126147

Gérard, F., Mayer, K. U., Hodson, M. J., and Ranger, J. (2008). Modelling the biogeochemical cycle of silicon in soils: application to a temperate forest ecosystem. *Geochimica Cosmochimica Acta* 72 (3), 741–758. doi:10.1016/j.gca.2007.11.010

Gilbert, D., Amblard, C., Bourdier, G., and Francez, A. J. (1998). The microbial loop at the surface of a peatland: structure, function, and impact of nutrient input. *Microb. Ecology* 35 (1), 83–93. doi:10.1007/s002489900062

Graham, J. D., Glenn, N. F., Spaete, L. P., and Hanson, P. J. (2020). Characterizing peatland microtopography using gradient and microform-based approaches. *Ecosystems* 23 (7), 1464–1480. doi:10.1007/s10021-020-00481-z

Graham, J. D., Ricciuto, D. M., Glenn, N. F., and Hanson, P. J. (2022). Incorporating microtopography in a land surface model and quantifying the effect on the carbon cycle. *J. Adv. Model. Earth Syst.* 14, e2021MS002721. doi:10.1029/2021ms002721

Hancock, M. H., Klein, D., Andersen, R., and Cowie, N. R. (2018). Vegetation response to restoration management of a blanket bog damaged by drainage and afforestation. *Appl. Veg. Sci.* 21, 167–178. doi:10.1111/avsc.12367

Harris, A., and Baird, A. J. (2019). Microtopographic drivers of vegetation patterning in blanket peatlands recovering from erosion. *Ecosystems* 22 (5), 1035–1054. doi:10.1007/s10021-018-0321-6

Heal, O. W. (1964). Observations on the seasonal and spatial distribution of testaceans (protozoa: rhizopoda) in *sphagnum*. *J. Animal Ecol.* 33, 395–412. doi:10.2307/2561

Hughes, H. J., Sondag, F., Cocquyt, C., Laraque, A., Pandi, A., André, L., et al. (2011). Effect of seasonal biogenic silica variations on dissolved silicon fluxes and isotopic signatures in the congo river. *Limnol. Oceanogr.* 56 (2), 551–561. doi:10.4319/lo.2011.56.2.0551

Jassey, V. E., Chiapusio, G., Mitchell, E. A., Binet, P., Toussaint, M. L., and Gilbert, D. (2011). Fine-scale horizontal and vertical micro-distribution patterns of testate amoebae along a narrow fen/bog gradient. *Microb. Ecol.* 61 (2), 374–385. doi:10.1007/s00248-010-9756-9

Katz, O., Puppe, D., Kaczorek, D., Prakash, N. B., and Schaller, J. (2021). Silicon in the soil–plant continuum: intricate feedback mechanisms within ecosystems. *Plants* 10 (4), 652. doi:10.3390/plants10040652

Keiser, A. D., Davis, C. L., Smith, M., Bell, S. L., Hobbie, E. A., and Hofmockel, K. S. (2025). Depth and microtopography influence microbial biogeochemical processes in a forested peatland. *Plant Soil* 509 (1), 833–846. doi:10.1007/s11104-024-06895-1

Kokfelt, U., Struyf, E., and Randsalu, L. (2009). Diatoms in peat–dominant producers in a changing environment? *Soil Biol. Biochem.* 41 (8), 1764–1766. doi:10.1016/j.soilbio.2009.05.012

Kokfelt, U., Struyf, E., Reuss, N., Sonesson, M., Rundgren, M., Skog, G., et al. (2010). Wetland development, permafrost history and nutrient cycling inferred from late Holocene peat and Lake sediment records in subarctic Sweden. *J. Paleolimnol.* 44, 327–342. doi:10.1007/s10933-010-9406-8

Leah, M., Wells, C., Huckerby, E., and Stamper, P. (1998). Lancaster: Lancashire Imprints. The Wetlands of Shropshire and Staffordshire.

Limpens, J., Berendse, F., Blodau, C., Canadell, J. G., Freeman, C., Holden, J., et al. (2008). Peatlands and the carbon cycle: from local processes to global Implications–A synthesis. *Biogeosciences* 5 (5), 1475–1491. doi:10.5194/bg-5-1475-2008

Lizoňová, Z., Zhai, M., Bojková, J., and Horsák, M. (2019). Small-scale variation of testate amoeba assemblages: the effect of site heterogeneity and empty shell inclusion. *Microb. Ecology* 77 (4), 1014–1024. doi:10.1007/s00248-018-1292-z

Lousier, J. D., and Parkinson, D. (1981). The disappearance of the empty tests of litter- and soil-testate amoebae (testacea, rhizopoda, protozoa). *Arch. für Protistenkd.* 124 (3), 312–336. doi:10.1016/s0003-9365(81)80024-3

Marcisz, K., Lamentowicz, L., Słowińska, S., Słowiński, M., Muszak, W., and Lamentowicz, M. (2014). Seasonal changes in sphagnum peatland testate amoeba communities along a hydrological gradient. *Eur. J. Protistology* 50, 445–455. doi:10.1016/j.ejop.2014.07.001

Mazei, Y. A., and Tsyganov, A. N. (2006). *Freshwater testate Amoebae*. Moscow: KMK Publisher. [in Russian].

Mazei, Y. A., and Tsyganov, A. N. (2007). Species composition, spatial distribution and seasonal dynamics of testate Amoebae community in a sphagnum bog (middle volga region, Russia). *Protistology* 5 (2-3), 156–206. doi:10.1134/s1062359007060131

Mazei, Y. A., Trulova, A., Mazei, N. G., Payne, R. J., and Tsyganov, A. N. (2020). Contributions of temporal and spatial variation to the diversity of soil-dwelling testate amoeba assemblages in a swampy forest. *Pedobiologia* 81, 150660. doi:10.1016/j.pedobi.2020.150660

Mitchell, E. A., Payne, R. J., and Lamentowicz, M. (2008). Potential implications of differential preservation of testate amoeba shells for paleoenvironmental reconstruction in peatlands. *J. Paleolimnol.* 40 (2), 603–608. doi:10.1007/s10933-007-9185-z

Mitchell, E. A. D., Buttler, A., Grosvernier, P., Rydin, H., Hoosbeek, M. R., Greenup, A., et al. (2000a). Relationships among testate amoebae (protozoa), vegetation and water chemistry in five *Sphagnum*-dominated peatlands in Europe. *New Phytol.* 145, 95–106. doi:10.1046/j.1469-8137.2000.00550.x

Mitchell, E. A. D., Borcard, D., Buttler, A. J., Grosvernier, P., Gilbert, D., and Gobat, J. M. (2000b). Horizontal distribution patterns of testate amoebae (protozoa) in a *Sphagnum magellanicum* carpet. *Microb. Ecol.* 39 (4), 290–300. doi:10.1007/s002489900187

Ogden, C. G., and Headley, R. H. (1980). *An atlas of freshwater testate amoebae*. Oxford: Oxford University Press.

Page, S., Hosciło, A., Wösten, H., Jauhiainen, J., Silvius, M., Rieley, J., et al. (2009). Restoration ecology of lowland tropical peatlands in southeast Asia: current knowledge and future research directions. *Ecosystems* 12, 888–905. doi:10.1007/s10021-008-9216-2

Payne, R. J., and Mitchell, E. A. D. (2009). How many is enough? Determining optimal count totals for ecological and palaeoecological studies of testate Amoebae. *J. Palaeolimnology* 42, 483–495. doi:10.1007/s10933-008-9299-y

Perryman, C. R., McCalley, C. K., Ernakovich, J. G., Lamit, L. J., Shorter, J. H., Lilleskov, E., et al. (2022). Microtopography matters: Belowground CH4 cycling regulated by differing microbial processes in peatland hummocks and lawns. *J. Geophys. Res. Biogeosciences* 127 (8), e2022JG006948. doi:10.1029/2022jg006948

Pickett, S. T. (1989). Space-for-time substitution as an alternative to long-term studies. in *Long-term studies in ecology: approaches and alternatives*. New York, NY: Springer New York.

Puppe, D. (2020). Review on protozoic silica and its role in silicon cycling. *Geoderma* 365, 114224. doi:10.1016/j.geoderma.2020.114224

Puppe, D., Kaczorek, D., Wanner, M., and Sommer, M. (2014). Dynamics and drivers of the protozoic Si pool along a 10-year chronosequence of initial ecosystem states. *Ecol. Eng.* 70, 477–482. doi:10.1016/j.ecoleng.2014.06.011

Puppe, D., Ehrmann, O., Kaczorek, D., Wanner, M., and Sommer, M. (2015). The protozoic Si pool in temperate forest ecosystems - quantification, abiotic controls and interactions with earthworms. *Geoderma* 243-244, 196–204. doi:10.1016/j.geoderma.2014.12.018

Puppe, D., Wanner, M., and Sommer, M. (2018). Data on euglyphid testate amoeba densities, corresponding protozoic silicon pools, and selected soil parameters of initial and forested biogeosystems. *Data Brief.* 21, 1697–1703. doi:10.1016/j.dib.2018.10.164

Puppe, D., Kaczorek, D., and Schaller, J. (2022). "Biological impacts on silicon availability and cycling in agricultural plant-soil systems," in *Silicon and nano-silicon in environmental stress management and crop quality improvement* (Academic Press), 309–324.

Qin, Y., Puppe, D., Payne, R., Li, L., Li, J., Zhang, Z., et al. (2020). Land-use change effects on protozoic silicon pools in the dajiuhu national wetland Park, China. *Geoderma* 368, 114305. doi:10.1016/j.geoderma.2020.114305

Qin, Y., Puppe, D., Zhang, L., Sun, R., Li, P., and Xie, S. (2021). How Does *Sphagnum* Growing Affect Testate Amoeba Communities and Corresponding Protozoic Si Pools? Results from Field Analyses in SW China. *Microb. Ecol.* 82, 459–469. doi:10.1007/s00248-020-01668-6

Qin, Y., Puppe, D., Li, H., Mazei, Y., Tsyganov, A. N., Man, B., et al. (2022). Peatland degradation in Asia threatens the biodiversity of testate amoebae (Protozoa) with consequences for protozoic silicon cycling. *Geoderma* 420, 115870. doi:10.1016/j.geoderma.2022.115870

Ragueneau, O., Varela, E. D. B., Tréguer, P., Quéguiner, B., and Del Amo, Y. (1994). Phytoplankton dynamics in relation to the biogeochemical cycle of silicon in a coastal ecosystem of Western Europe. *Mar. Ecol. Prog. Ser.* 106, 157–172. doi:10.3354/meps106157

Roe, H. M., Elliott, S. M., and Patterson, R. T. (2017). Re-assessing the vertical distribution of testate amoeba communities in surface peats: implications for palaeohydrological studies. *Eur. J. Protistology* 60, 13–27. doi:10.1016/j.ejop.2017.03.006

Rydin, H., and Jeglum, J. K. (2013). *The biology of peatlands*. Oxford, UK: Oxford University Press.

Schaller, J., Puppe, D., Kaczorek, D., Ellerbrock, R., and Sommer, M. (2021). Silicon cycling in soils revisited. *Plants* 10 (2), 295. doi:10.3390/plants10020295

Shukla, T., Tang, W., Trettin, C. C., Chen, G., Chen, S., and Allan, C. (2023). Quantification of microtopography in natural ecosystems using close-range remote sensing. *Remote Sens.* 15, 2387. doi:10.3390/rs15092387

Sommer, M., Jochheim, H., Höhn, A., Breuer, J., Zagorski, Z., Busse, J., et al. (2013). Si cycling in a forest biogeosystem – the importance of transient state biogenic Si pools. *Biogeosciences* 10, 4991–5007. doi:10.5194/bg-10-4991-2013

Struyf, E., and Conley, D. J. (2009). Silica: an essential nutrient in wetland biogeochemistry. *Front. Ecol. Environ.* 7 (2), 88–94. doi:10.1890/070126

Struyf, E., and Conley, D. J. (2012). Emerging understanding of the ecosystem silica filter. *Biogeochemistry* 107 (1), 9–18. doi:10.1007/s10533-011-9590-2

Struyf, E., Smis, A., Van Damme, S., Garnier, J., Govers, G., Van Wesemael, B., et al. (2010a). Historical land use change has lowered terrestrial silica mobilization. *Nat. Communications* 1 (1), 129. doi:10.1038/ncomms1128

Struyf, E., Mörth, C. M., Humborg, C., and Conley, D. J. (2010b). An enormous amorphous silica stock in boreal wetlands. *J. Geophys. Res. Biogeosciences* 115 (G4). doi:10.1029/2010jg001324

Sullivan, M. E., and Booth, R. K. (2011). The potential influence of short-term environmental variability on the composition of testate amoeba communities in sphagnum peatlands. *Microb. Ecol.* 62 (1), 80–93. doi:10.1007/s00248-011-9875-y

Swindles, G. T., Green, S. M., Brown, L., Holden, J., Raby, C. L., Turner, T. E., et al. (2016). Evaluating the use of dominant microbial consumers (testate amoebae) as indicators of blanket peatland restoration. *Ecol. Indic.* 69, 318–330. doi:10.1016/j.ecolind.2016.04.038

Tanneberger, F., Appulo, L., Ewert, S., Lakner, S., Ó Brolcháin, N., Peters, J., et al. (2020). The power of nature-based solutions: how peatlands can help us to achieve key EU sustainability objectives. *Adv. Sustain. Syst.* 5, 2000146. doi:10.1002/adsu.202000146

Tréguer, P. J., and De La Rocha, C. L. (2013). The world ocean silica cycle. *Annu. Review Marine Science* 5 (1), 477–501. doi:10.1146/annurev-marine-121211-172346

Wanner, M., Elmer, M., Kazda, M., and Xylander, W. E. (2008). Community assembly of terrestrial testate amoebae: how is the very first beginning characterized? *Microb. Ecol.* 56 (1), 43–54. doi:10.1007/s00248-007-9322-2

Wanner, M., Elmer, M., Sommer, M., Funk, R., and Puppe, D. (2015). Testate Amoebae colonizing a newly exposed land surface are of airborne origin. *Ecol. Indic.* 48, 55–62. doi:10.1016/j.ecolind.2014.07.037

Warner, B. G., Asada, T., and Quinn, N. P. (2007). Seasonal influences on the ecology of testate amoebae (protozoa) in a small sphagnum peatland in southern Ontario, Canada. *Microb. Ecology* 54 (1), 91–100. doi:10.1007/s00248-006-9176-z

Wehrhan, M., Puppe, D., Kaczorek, D., and Sommer, M. (2021). Spatial patterns of aboveground phytogenic Si stocks in a grass-dominated catchment – results from UAS based high resolution remote sensing. *Biogeosciences* 18, 5163–5183. doi:10.5194/bg-18-5163-2021

Wilkinson, D. M., and Mitchell, E. A. (2010). Testate amoebae and nutrient cycling with particular reference to soils. *Geomicrobiol. J.* 27 (6-7), 520–533. doi:10.1080/01490451003702925

Zaman, W., Ayaz, A., and Puppe, D. (2025). Biogeochemical cycles in plant–soil systems: significance for agriculture, interconnections, and anthropogenic disruptions. *Biology* 14 (4), 433. doi:10.3390/biology14040433

Zhou, L., Fan, J., Li, R., Vachula, R. S., and Xu, B. (2025). Seasonal variations of dissolved silicon in a karst bamboo forest soil-plant system. *Catena* 257, 109139. doi:10.1016/j.catena.2025.109139